

# An improved methodology to evaluate crop salt tolerance from field trials

G. van Straten<sup>a,\*</sup>, A.C. de Vos<sup>b</sup>, J. Rozema<sup>c</sup>, B. Bruning<sup>d</sup>, P.M. van Bodegom<sup>e</sup>



<sup>a</sup> Department of Biobased Chemistry and Technology, Wageningen University, P.O. Box 17, 6700 AA, Wageningen, The Netherlands

<sup>b</sup> Salt Farm Texel, Mokweg 41, 1797 SB Den Hoorn, The Netherlands

<sup>c</sup> Faculty of Science, Department of Ecological Science, Section Systems Ecology, Free University Amsterdam, De Boelelaan 1085, 1081 HV Amsterdam, The Netherlands

<sup>d</sup> Salt Farm Texel & Salt Farm Foundation, Mokweg 41, 1797 SB Den Hoorn, The Netherlands

<sup>e</sup> Department Environmental Biology, Institute of Environmental Sciences, Leiden University, Einsteinweg 2, 2333 CC Leiden, The Netherlands

## ARTICLE INFO

### Keywords:

Crop salinity tolerance  
Parameter estimation  
Salinization

## ABSTRACT

The salt tolerance of crops is commonly expressed in descriptive parameters such as threshold or 50%-yield soil salinity and shape parameters describing the yield curve. Estimation by visual or simplified ordinary least squares (OLS) regression methods has multiple issues: parameter bias due to uncertainty in soil salinity, lack of independent estimates of the reference yield, questionable robustness of the threshold parameter and missing information about uncertainty and correlation of the parameter estimates. Here, we present a comprehensive OLS method together with an analysis of its statistical properties to alleviate and overcome such issues, on the basis of a numerical experiment that mimics observed yield responses to saline groundwater across a range of salinities in the experimental test facility Salt Farm Texel.

The results indicate under which experimental conditions bias is not a major problem. The method allows estimation of the zero-observed-effect yield from the data, which is relevant to agricultural practice. Estimates for zero-observed-effect yield and threshold E<sub>Ce</sub> are negatively correlated, underlining the difficulty of obtaining reliable threshold values. The estimated confidence regions are reliable and robust against soil salinity uncertainty, but large observation error jeopardizes the confidence intervals, especially for the slope parameter. Data uncertainty alone can be responsible for substantial differences from experiment to experiment, providing a partial explanation for the wide variety in reported parameters in the literature, and stressing the need for long-term repetitions.

Given the lack of robustness of the threshold parameter, we propose to adopt the 90%-yield EC (EC<sub>e90</sub>) as tolerance parameter. Its confidence bounds can be obtained from a simple reformulation of the original models. We also present uncertainty ellipses as a suitable tool to unite multiple-year estimates. The method is offered as a solid and generic basis for reliable assessment of the cultivation potential of varieties and crops on salt-affected soils.

## 1. Introduction

One of the most common representations of salt tolerance originates back to the celebrated Maas-Hoffman model (Maas and Hoffman, 1977) describing crop salt tolerance by a threshold salinity parameter below which yield is not affected, and a slope parameter describing the decline in relative yield when salinity is beyond the threshold.

Previous work (Ulery et al., 1998), as well as a recent study (Stuyt et al., 2016) reveals an extremely wide uncertainty range in crop salinity tolerance parameters. Many studies report the estimates without due account to the uncertainties associated with the estimation. Also, the existence of a real threshold has been debated, leading to alternate

S-shape models, such as the models by Van Genuchten and Hoffman (1984) and Van Genuchten and Gupta (1993). Though probably agronomical more correct, these models have found less wide application, as the parameters do not have the same intuitive appeal as the parameters of the threshold model.

While Van Genuchten and Hoffman (1984) did an extensive study on various least squares methods to estimate the parameters of either model from soil salinity versus yield data, a number of issues need further attention. We focus on: (i) possible bias due to uncertainty in the independent variable (soil salinity), (ii) the assessment of parameter uncertainty and correlation, (iii) the consequences of measurement noise and parameter correlation to the variability of tolerance estimates

\* Corresponding author.

E-mail addresses: [gerrit.vanstraten@wur.nl](mailto:gerrit.vanstraten@wur.nl) (G. van Straten), [adevos@saltfarmtexel.nl](mailto:adevos@saltfarmtexel.nl) (A.C. de Vos), [j.rozema@vu.nl](mailto:j.rozema@vu.nl) (J. Rozema), [bbruning@saltfarmtexel.nl](mailto:bbruning@saltfarmtexel.nl) (B. Bruning), [p.m.van.bodegom@cml.leidenuniv.nl](mailto:p.m.van.bodegom@cml.leidenuniv.nl) (P.M. van Bodegom).

<https://doi.org/10.1016/j.agwat.2018.09.008>

Received 17 July 2018; Received in revised form 26 August 2018; Accepted 3 September 2018

0378-3774/© 2018 The Authors. Published by Elsevier B.V. This is an open access article under the CC BY license (<http://creativecommons.org/licenses/by/4.0/>).

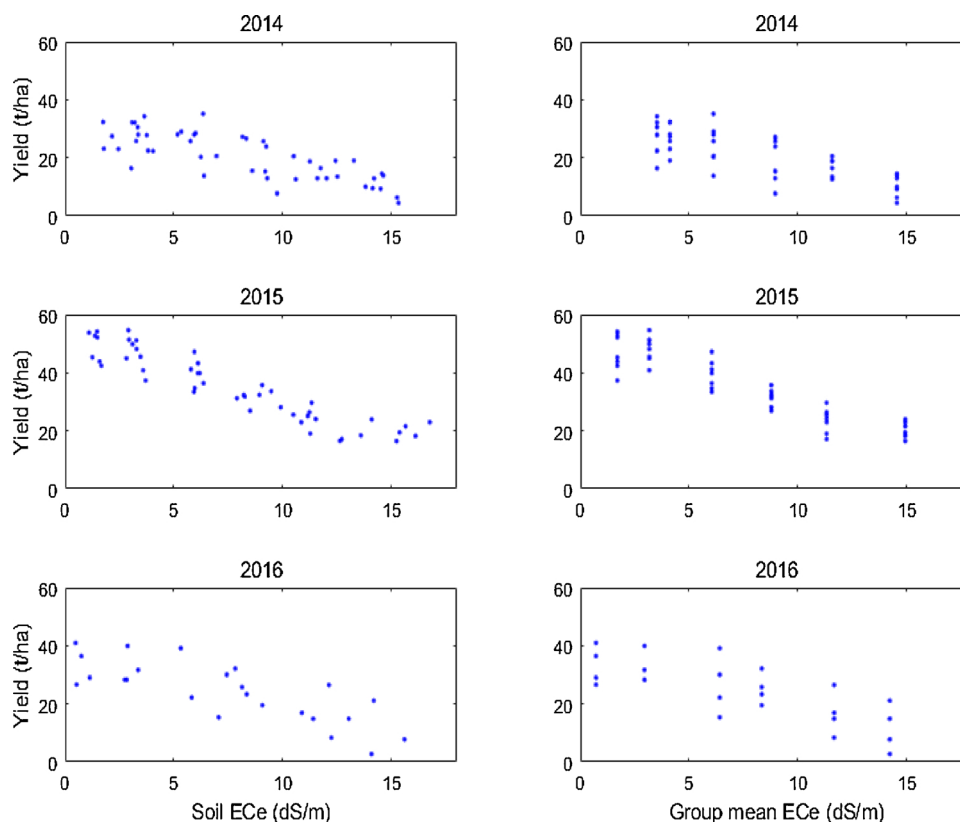


Fig. 1. Sample data from Salt Farm Texel (potato Achilles, years 2014–2016). Tuber yield versus seasonal mean soil salinity as saturated paste. Left hand side: each replicate (8 in 2014, 2015, 4 in 2016) plotted separately. Right hand side: against the group mean.

between experiments, (iv) whether a different parameterization can be found that is more independent of the chosen model.

The motivation for the current study is that the worldwide expansion of salinization stimulates the quest for relatively salt tolerant varieties to provide a partial solution (Ghassemi et al., 1995; Qadir et al., 2014; Rozema and Flowers, 2008; Rozema et al., 2015). Therefore it is necessary to have a solid estimation method that, ultimately, allows for a reliable assessment of the suitability of varieties and crops for cultivation on salt-affected soils.

## 2. Models and data for investigating salt tolerance of crops

### 2.1. Typical uncertainties in crop yields in response to soil salinity

Before proceeding we first present some typical crop data to provide an impression of the uncertainties involved.

Fig. 1 shows three consecutive years of a series of data over the years 2012–2017 of field experiments conducted at Salt Farm Texel, (SFT). SFT has a facility of 1 ha split-up in 56 fields, grouped in 8 randomly selected fields that receive irrigation with one of seven irrigation Electric Conductivities (ECs) in a rotational system with one or two irrigation events per day. The irrigation water is obtained by controlled mixing of fresh dune water with sea water. The target irrigation ECs are 0, 4, 8, 12, 16, 20 and 32 dS/m. In this paper, data from EC = 32 are not considered, as it did not lead to consistent yields. The actual EC of the lowest level was 1.7 dS/m up till 2015, which did not allow estimating a zero-observed-effect (or reference) yield. An EC of 0.5 dS/m was achieved from 2016 onwards, but even such small salinity deviations may cause deviation from a zero-observed-effect yield (below, we will show how this problem can be circumvented by considering the reference yield as a parameter estimated from the data). Soil samples and soil water samples were taken at various times during the growing season at three depths around the root zone, from which

the seasonal mean soil salinity (measured as the Electric Conductivity of a soil saturated paste; ECe) is derived per field as used in the Fig. 1 (left). In Fig. 1 (right), the data have been plotted again against the seasonal mean ECe per treatment group. Based on the water and salt balance, the expected pore water conductivity was 1–2 percent higher than the irrigation EC (depending on the year). Together with the experimentally established relationship between ECe and pore water EC (ECe = 0.69 pore water EC), it is deduced that the expected values for the remaining 6 group treatment means are about 1.2, 2.8, 5.6, 8.4, 11.2 and 14 dS m<sup>-1</sup>. Details of the irrigation and sampling procedure can be found in De Vos et al. (2016) and Van Straten et al. (2016).

Fig. 1 shows how, at SFT, the reproducibility and consistency of the irrigation and sampling improved over the years, as seen from the more clustered data in later years, and the more even distribution of the group means over the soil salinity range. In particular, by the installation of a tap water basin in 2016, SFT provided lower EC values of irrigation water. Moreover, the group mean ECe gets closer to the target ECe's. This does not disqualify the soil salinity – yield pairs (left panels of Fig. 1) as useful points for the determination of the tolerance curve; it only means that the true soil salinity was not the one that was originally intended. Even in 2016 though, there is considerable scatter in yields for fields supposed to have the same treatment. Also average yields vary from year to year.

In general salinity effects on crop yield can be described by a multiplicative limitation function, i.e.

$$Y = Y_o f(EC_e; \beta) \quad (1)$$

where

$Y$  actual salt affected yield  
 $Y_o$  yield without salinity limitation (but possibly affected by other factors); reference or zero-observed-effect yield  
 $f$  limit function, between 1 (no effect) and 0 (complete mortality)  
 $EC_e$  soil salinity, expressed as saturated paste

$\beta$  a vector of parameters in the function  $f$ .

Any set of consistent units can be chosen. The common practice to estimate parameters  $\beta$  from relative yield data  $Y/Y_0$  implies that valid results are only obtained in the rare case that the zero-observed-effect yield has been measured with high precision.

There might be interaction between salt tolerance and evapotranspiration of some crops, e.g. Groenvelde et al. (2013); Shani and Dudley (2001); Sadeh and Ravina (2000). The literature is not decisive on this point and further study is needed to see whether this is consistent with the simple formulation in Eq. (1). Here we adhere to the dominant approach in the salt tolerance literature and base our investigations on two common salt tolerance models.

## 2.2. Common salt tolerance models

### 2.2.1. The threshold model

The threshold (or breakpoint) model by Maas and Hoffman (1977), denoted in the sequel as *MH*, is given by

$$Y = \begin{cases} Y_0 & ECe \leq ECe_{thr} \\ Y_0 + S*(ECe - ECe_{thr}) & ECe_{thr} < ECe < ECe_{thr} - \frac{Y_0}{S} \\ 0 & ECe > ECe_{thr} - \frac{Y_0}{S} \end{cases} \quad (2)$$

where

$Y$  yield at a particular  $ECe$  (dependent variable)

$Y_0$  yield without saline stress (a parameter)

$ECe_{thr}$  threshold (breakpoint)  $ECe$  beyond which yield effects are expected (a parameter)

$S$  slope, i.e. the loss in yield per unit  $ECe$  beyond the threshold (a parameter).

The yield is expressed in appropriate yield units (possibly different by crop), and the  $ECe$  is expressed in  $dS\ m^{-1}$ . The slope in the equation above is negative, and is expressed in appropriate yield units per  $dS\ m^{-1}$ . Note that in the *MH* model there is a discontinuity in the derivative of the yield to  $ECe$  at  $ECe = ECe_{thr}$ . In the *MH* model, the number of parameters to be estimated is 3.

Once an estimate of the unaffected yield  $\hat{Y}_0$  is available, in addition to the estimates  $\hat{ECe}_{thr}$  and  $\hat{S}$ , a plot in terms of percentage of unaffected yield can be presented as

$$\frac{Y}{\hat{Y}_0} (\%) = \begin{cases} 100 & ECe \leq \hat{ECe}_{thr} \\ 100 + \hat{S}_{\%}*(ECe - \hat{ECe}_{thr}) & \hat{ECe}_{thr} < ECe < \hat{ECe}_{thr} - \frac{100}{\hat{S}_{\%}} \\ 0 & ECe > \hat{ECe}_{thr} - \frac{100}{\hat{S}_{\%}} \end{cases} \quad (3)$$

where

$\hat{S}_{\%} = 100 \hat{S} / \hat{Y}_0$  the percentage yield loss per unit of  $dS/m$  beyond the threshold (relative slope).

Obviously the relative slope curve relies on the estimates of both slope and zero-observed-effect yield. The latter is unknown in real field situations, but is often derived from the yields observed at the lowest salinity level. From the above it is clear that this procedure is prone to errors.

### 2.2.2. The S-shape model

One particular useful form of an S-shape model is presented in Van Genuchten and Hoffman (1984) as

$$Y = Y_0 \frac{1}{1 + \left(\frac{ECe}{ECe_{50}}\right)^p} \quad (4)$$

where the additional symbols are

$ECe_{50}$  the  $ECe$  at which the yield has dropped to 50% of the maximum yield  $Y_0$  (parameter)  $p$  a dimensionless steepness parameter.

This, too, is a three-parameter model. In a later study, Van Genuchten and Gupta (1993) found that fixing the value of  $p$  to 3,

resulted in only slightly worse fits for most crops. By doing that, the number of parameters to be estimated reduces to 2.

Once an estimate of the unaffected yield  $\hat{Y}_0$  is available, in addition to the estimates  $\hat{ECe}_{50}$  and  $\hat{p}$  a plot in terms of percentage of unaffected yield is given by

$$\frac{Y}{\hat{Y}_0} (\%) = 100 \frac{1}{1 + \left(\frac{ECe}{\hat{ECe}_{50}}\right)^{\hat{p}}} \quad (5)$$

In contrast to the *MH* model, the parameters in the relative plot remain the same, irrespective of the estimate of unaffected yield  $\hat{Y}_0$ . Also, there are no discontinuities in the derivative of the yield to  $ECe$ .

Hence, from a mathematical point of view, the S-shape model is preferable. However, in agricultural practice, the *MH* model has the charm of an easy interpretation.

## 2.3. Parameter estimation

There are various methods to estimate abovementioned parameters from data. A linear equation can be fit for salinities beyond the threshold by the least squares method (Maas and Hoffman, 1977). This method requires a visual determination of the threshold and the reference yield. In the example of Fig. 1, visual inspection would suggest that, if a threshold  $ECe$  exists at all (cf. the 2015 data), it must be between 4 and 6  $dS\ m^{-1}$ . This uncertainty will affect the result. In Maas (1993) it was stated that the threshold can be found by the intersection of a horizontal and sloping regression line, but this does not eliminate the arbitrariness as the location of the horizontal line will depend on the number of points included. As more objective procedure Van Genuchten and Hoffman (1984) proposed to apply ordinary least squares (OLS), solved by a non-linear optimization method. This is also the basis for our study, but expanded with an in-depth analysis and the assessment of parameter confidence regions and correlations.

The OLS method assumes that the independent variable – soil  $ECe$  – is known with large precision. This is obviously not the case, as clearly testified in Fig. 1. Hence the problem is a so-called errors-in-variables case (also known as type 2 errors in statistical literature), leading to biased estimates, meaning that the mean of the estimates over repeated experiments will not converge to the true value. Rather than taking resort to instrumental variables or total least squares, requiring additional assumptions, we keep the attractive OLS method, and just test by a numerical Monte Carlo experiment the bias under realistic noise conditions.

Such evaluation of the OLS estimation is not complete without the assessment of parameter uncertainties and the correlation between the estimates. From Eq. (2), it is apparent that a higher estimate for the reference yield must be compensated by a lower estimate of the threshold  $ECe$ . This alone can be a source of variation in reported threshold values.

The parameter estimation method and the assessment of the covariance of the parameters is outlined in Appendix A. The method was implemented in matlab, allowing to analyse the structure of the parameter solutions in more detail, but it can also be done in standard statistical packages such as SPSS.

## 2.4. The numerical experiment

The OLS method applied to an individual year provides estimates of the parameters and of the (co-)variance of the estimated parameters, but the asymptotic properties of the estimator can only be judged over a large number of experiments. Hence a numerical experiment was set up pretending the availability of a large number of datasets with known, fixed parameters. The experiment was set up in so that it mimics the observed situation as closely as possible. The unparalleled rigour and gain in experience of the experiments at SFT allowed to suspect that part of the variation in soil salinity is real, due to variations in

irrigation, especially in earlier years. Generally, especially regarding literature data, it is impossible to tell whether the variation of observed ECe in the soil is real or the result of observation and sampling error, or both. Therefore, in the numerical experiments, sets of artificial data were generated with a varying distribution of the two uncertainties over the total. The standard deviation of the soil EC due to uncertainties in the transfer from irrigation to soil is called  $sdX_{target}$ , and the observation and sampling error is called  $sdX$ . There is also uncertainty in the yield,  $sdY$ .

Starting with the irrigation EC of the six treatments, the target soil ECe was computed following information in section 2.1. Next, 100 artificial data sets each with 48 ( $8 \times 6$ ) ECe-yield pairs were generated in two steps. First, random normally distributed noise with standard deviation (s.d.)  $sdX_{target}$  was added to the target soil ECe's, thus representing the true variation in the soil. Next, with the model and a set of realistic parameters (MH:  $Y_0 = 60 \text{ tons ha}^{-1}$ ,  $ECe_{thr} = 4 \text{ dS m}^{-1}$ ,  $S = -3 \text{ tons ha}^{-1} \text{ dS m}^{-1}$ ; vGH:  $Y_0 = 60 \text{ tons ha}^{-1}$ ,  $ECe_{50} = 10 \text{ dS m}^{-1}$ ,  $p = 3$ ) the yield was computed for each true soil ECe. Finally, normally distributed observation noise was added to both the soil ECe (with s.d.  $sdX$ ) as well as the yield (with s.d.  $sdY$ ). We set  $sdY$  to 4 tons/ha. This gives an individual 95% realization range of 16 tons/ha (cf. Figs. 1 and 4). The s.d. of the target ECe and the ECe observation noise was varied between 0 and 3 dS/m. In this way, several sets of 100 virtual experiments were obtained for various distributions of the total noise in soil ECe over a true variation and a variation due to observation error. The data were specific for SFT, but it is important to stress that the procedure is generic for most salt tolerance of crops literature for which data consist of noisy ECe versus noisy yield data, e.g. De Pascale and Barbieri (1995).

### 3. Results and discussion

#### 3.1. Estimation and uncertainties in soil tolerance on real data; illustrative example

Fig. 2 shows the actually observed standard deviation of the seasonal mean soil ECe per treatment group in the various years and the improvement of the reproducibility over the years as a consequence of improved skills and experience at SFT. Thus, the high end of the chosen ECe noise is representative for the early years, and the low end for later years. There is also some variation of the noise between irrigation groups, but for simplicity, in the numerical experiment, the uncertainty has been set equal over all irrigation groups.

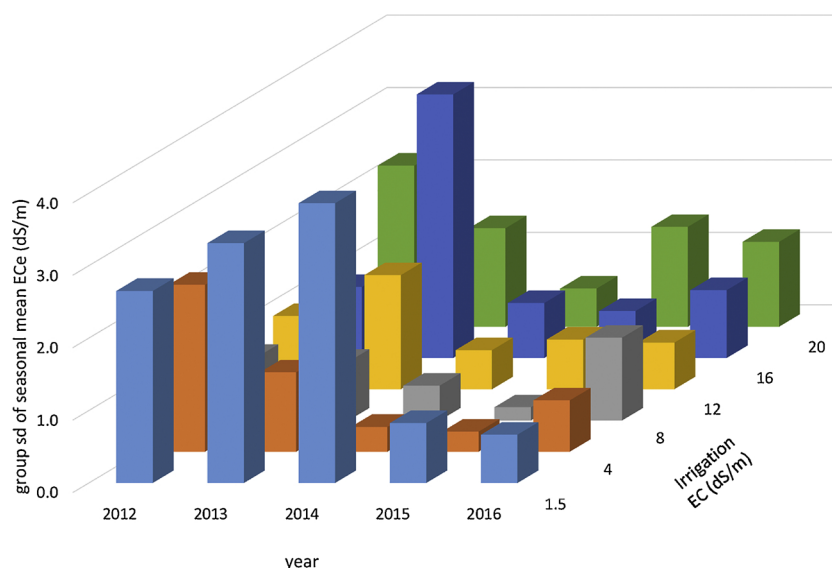


Fig. 2. Standard deviation of the seasonal mean soil ECe at Salt Farm Texel in various years for the different irrigation treatments.

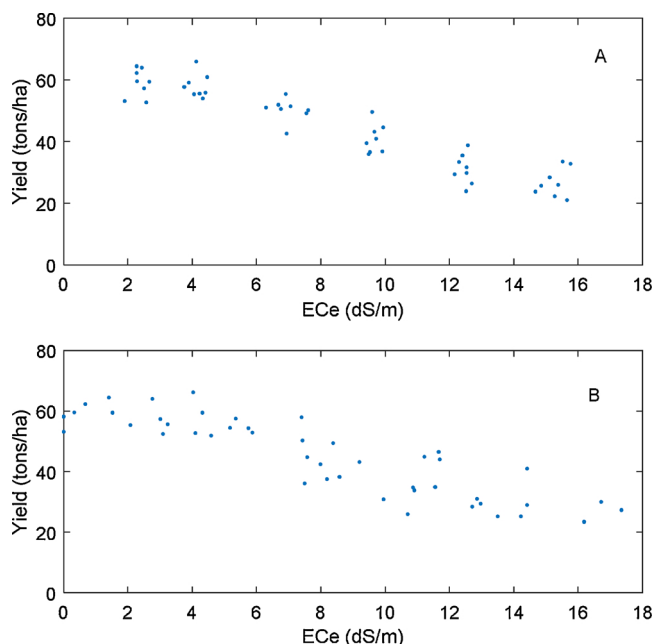
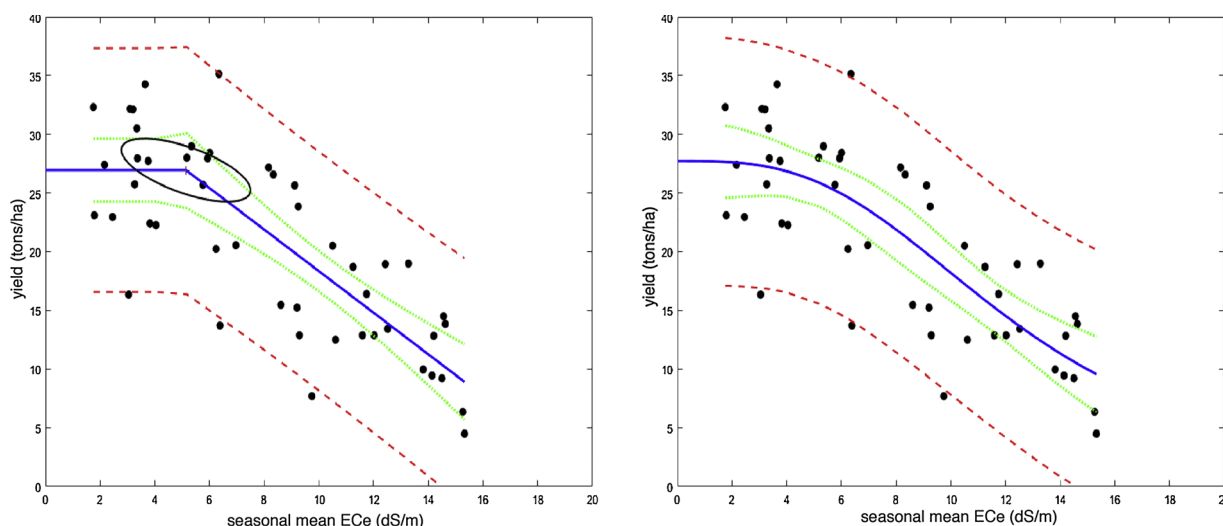


Fig. 3. Example of the effect of noise on generated artificial data (set 84 out of 100). A:  $sdX_{target} = 0.2$ ,  $sdX = 0.2$ ; B:  $sdX_{target} = 1$ ,  $sdX = 2$ ; in both cases  $sdY = 4$ .

To corroborate the realism of the artificial data, one sample out of the 100 artificial data sets is shown (Fig. 3) for different values of the target and observation noise in ECe. When the total noise is low (case A, sum 0.4 dS/m), the data become more clustered - resembling the 2015 situation -, whereas if the noise is large (case B, sum = 3 dS/m), the data look more distributed (resembling the 2014 situation).

In order to better understand the numerical experiment, it is appropriate to illustrate the estimation method. Achilles 2014 is taken as an example. The OLS fits and uncertainty bounds are shown in Fig. 4 and Table 1.

The individual prediction error bounds specify the range of outcomes for a single field subject to a specific soil salinity, e.g. at an ECe of 8 dS/m the yield will be between about 10 and 30 tons/ha. The simultaneous prediction error represents with 95% probability the mean outcome for a group of farmers or fields (in the example between 20 .



**Fig. 4.** Potato cultivar ‘Achilles’, 2014, MH (left) and vGH (right). Solid line: fit; dotted lines (inner bounds): simultaneous prediction error; dashed lines (outer bounds): prediction error for an individual measurement. Ellipse: 2-D cross section of the 95% confidence contour for  $Y_0$  and  $EC_{e_{thr}}$  (see text).

**Table 1**  
Estimates of salt tolerance using the OLS fits. Example for Achilles 2014.

Achilles 2014	MH			vGH		
	estimate	95% confidence interval		estimate	95% confidence interval	
		low	high		low	high
$EC_{e_{thr}}$ ( $dS\ m^{-1}$ )	5.13	2.77	7.50			
$S$ ( $tons\ ha^{-1}\ m\ dS^{-1}$ )	-1.77	-2.30	-1.24			
$EC_{e_{50}}$ ( $dS/m$ )				12.38	10.70	14.06
$p$ (-)				3.02	1.34	4.70
$Y_0$ ( $tons\ ha^{-1}$ )	26.95	24.27	29.63	27.73	24.48	30.99

The representation in Table 1 can be somewhat misleading since the correlation between parameter estimates was not accounted for. At each individual point the OLS provides an estimate of the co-variance, i.e. of the confidence contour around that point (and can also be obtained from the correlation matrix (not shown)). Fig. 5 shows that the center of the ellipse is located at the best estimate. The estimate for the threshold ECe is between 2.8 and 7.5  $dS\ m^{-1}$ , and that of the unaffected yield between 24 and 30  $tons\ ha^{-1}$ , in accordance with the standard representation in Table 1, but the combinations (2.8, 24) or (7.5, 30), for instance, are outside the confidence contour. Also, a high estimate

of the unaffected yield implies a low estimate of the threshold, and vice versa, illustrating one of the difficulties of obtaining reliable salt tolerance parameters from field data.

In addition to the default parameters, one can also obtain the  $EC_{e_{90}}$ , i.e. the ECe where the yield is 90% of the maximum yield, and the  $EC_{e_{50}}$ , representing the 50% yield ECe. The  $EC_{e_{90}}$  is 6.6 and 6.0  $dS\ m^{-1}$ , for MH and vGH, respectively, whereas the  $EC_{e_{50}}$  is 12.7 and 12.4  $dS\ m^{-1}$ , respectively. In this regard, the models yield similar values for properties that are of agricultural interest.

Table 2 presents the goodness of fit criteria of the two models (as defined in Appendix A), compared with simple linear regression (LR). The differences in root mean square error of the three models is hardly discernible. The MH model has the lowest sum of squares and the highest  $R^2$  values, although the differences are small. The addition of the extra parameter in the MH and vGH models compared to linear regression leads to a lower AIC, meaning that these more complex models are justified. This is in line with what is seen from the data of other years, and data from the literature. The ability to distinguish between MH and vGH will largely depend upon the availability of data at the high-end tail of the curve, but the agricultural significance of this part of the curve is low. The  $R^2$  values are rather low, in line with the high variation in yields. An analysis of the residuals (not shown) does not reveal correlation or skewness, meaning that the models are reasonable.

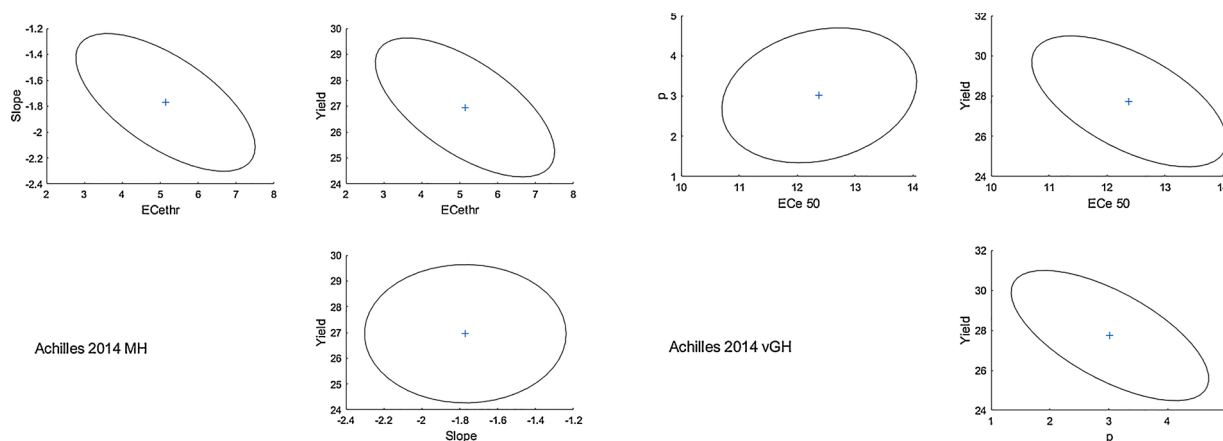


**Fig. 5.** Approximate 95% parameter confidence contours for all three parameter combinations, potato Achilles 2014. left: MH, right: vGH.



**Table 2**  
Goodness of fit of the 3 models, with Achilles 2014 as an example. Abbreviations: see Appendix A4.

goodness of fit	MH	vGH	LR	
ssq	1133.1	1150.0	1200.3	(tons/ha) <sup>2</sup>
df	45	45	46	–
RMSE	5.02	5.06	5.11	tons/ha
R <sup>2</sup>	0.63	0.62	0.60	–
R <sup>2</sup> _adj	0.61	0.61	0.60	–
AIC	343.6	344.3	344.4	–

3.2. Bias and reliability of confidence contours

The OLS method provides descriptive statistics for the estimate of an individual year, but for the generic behaviour of the estimator, the numerical experiment is instrumental. Fig. 6 shows the position of the individual estimates for the 100 realizations, with the same relatively large noise as in Fig. 3B. One of these points belongs to the artificial data of Fig. 3B.

It is striking that, across all realizations, the range of estimates in the ensemble (Fig. 6) closely resembles the shape of the estimated confidence contours of an individual estimate, including the correlation between estimates (Fig. 5). However, the true value barely falls within the range, indicating a clear bias in this case. This means that over a number of experiments the mean will be off from the true value. The noise for Fig. 6 was chosen to be rather high to clearly visualize the occurrence of bias. Similar plots can be presented for cases when the noise is smaller. In those cases, bias may be almost absent. The relation between noise and bias is further discussed in section 3.4.

In a situation without errors-in-variables the 2σ-bound represents the exact 95% confidence interval for linear parameters (such as Y<sub>0</sub>) and approximately 95% for non-linear parameters. When these conditions are not met, as is the case here, no firm statements can be made. To test whether the assumption was approximately valid, the distribution of the distance of the estimated point to the true point was tested, normalized by the estimated standard deviation, i.e.

$$\frac{|\hat{\beta} - \beta_{true}|}{\hat{\sigma}_{\beta}}$$

is evaluated. The result is shown in Fig. 7, for both the ‘high noise’ example as well as a ‘low noise’ one.

The statistics of the confidence intervals of both the estimates of ECe<sub>thr</sub> as well as Y<sub>0</sub> are close to the expectation that there are no more than 5 out of 100 cases where the true value is outside the 2-σ bound (α = 2), even if the noise is relatively large. Obviously, for an individual year, there is no guarantee that the true parameter is within the estimated uncertainty bound, underlining again the importance of repeated experiments. If the noise is large, Fig. 7 top reveals that the estimated confidence range of the slope is unreliable as more than 30% of the cases lies outside the 2-σ bound, or, formulated differently, the 2-σ bound is associated with a confidence level of about 70% rather than 95%. The difference disappears if the noise becomes smaller (Fig. 7, bottom).

3.3. Effects of taking group means on salt tolerance estimates

It is expected that the bias due to high noise in the soil salinity can be reduced by taking the mean of the treatment group prior to the estimation. Comparing Fig. 8 with Fig. 6 reveals that this is, indeed, the case.

This can be explained by the fact that in the presence of large observation noise the mean soil salinity is a better estimate of the actual soil salinity than the individual salinities per replicate. However, averaging may be counter-productive if the variation in the soil is largely determined by true variations in irrigation conditions (See section 3.4).

Averaging might also help to improve the confidence estimation statistics. Fig. 1 Regarding the ‘high noise’ case, the number of cases where the 2-σ bound is not met reduces from 33 to 20 out of 100 for the slope, which is an improvement, but still far from the ideal 5%. Averaging somewhat worsens the reliability of the confidence contour for ECe<sub>thr</sub> (from 4 cases out of 100 to 8), whereas the confidence contour of the zero-observed-effect yield (Y<sub>0</sub>) remains reliable. The latter probably

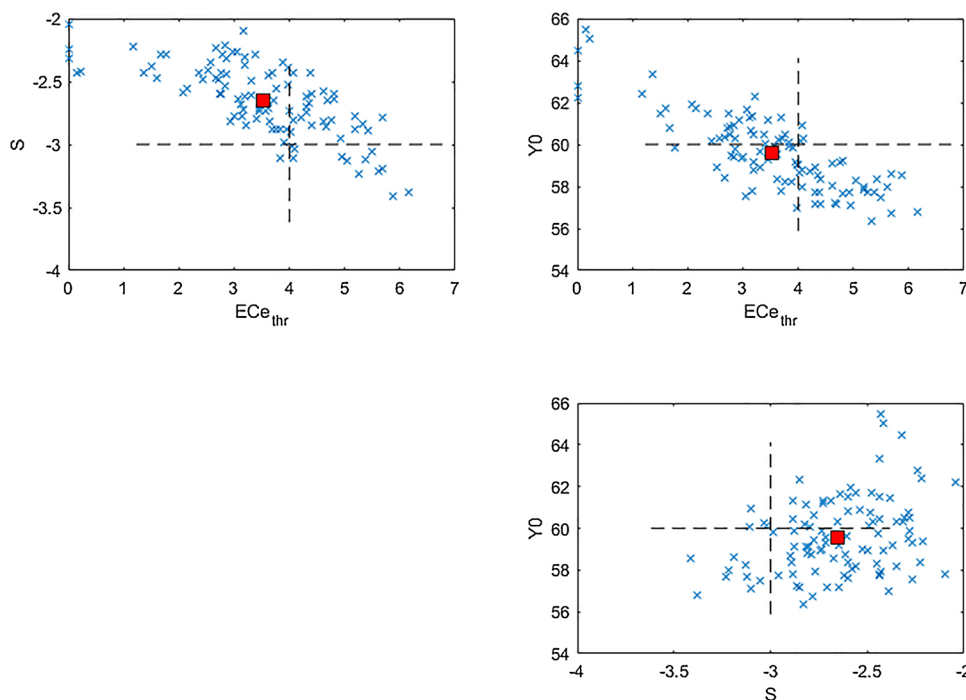


Fig. 6. The estimates for the 100 random artificial datasets with sdXtarget = 1, sdX = 2 and sdY = 4. The cross-hair represents the true point while the square shows the arithmetic means.

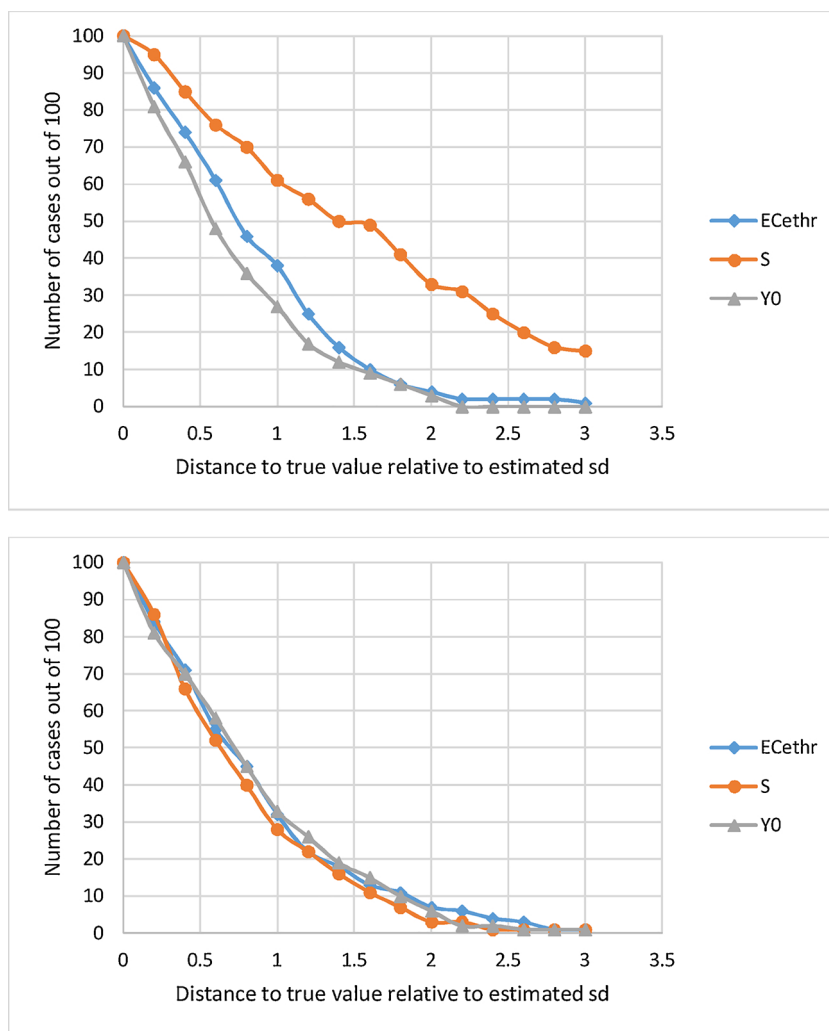


Fig. 7. The percentage of occurrences where the distance between estimate and true value relative to the standard deviation is larger than the value along the x-axis. Top: 'high noise'  $sdX_{target} = 1$ ,  $sdX = 2$ ; Bottom: 'low noise'  $sdX_{target} = 0.2$ ,  $sdX = 0.2$ .

relates to the fact that the models are linear in this parameter.

### 3.4. Effect of the distribution over target $E_{Ce}$ and observation $E_{Ce}$

In order to further study the effect of the two sources of noise in the soil  $E_{Ce}$ , the bias was studied as function of the distribution of the total noise over the irrigation target noise and the observation/sampling noise. We expect the bias to be larger if the proportion of the observation noise becomes larger. In that case, averaging over all replicates prior to estimation may be better. On the other hand, if the soil salinity is determined by variation in irrigation or in other soil properties (target noise), then the variation is real, and it is expected that averaging will not improve the estimates.

In general, this picture is confirmed in Fig. 9 where the bias is expressed as percentage of the true parameter value. A large proportion of observation noise causes a large bias in both  $E_{Ce_{thr}}$  as well as in  $S$ , while the bias in zero-observed-effect yield  $Y_0$  remains small. Beyond a contribution of observation noise of around 30%, averaging reduces the bias. Without observation noise, the bias is zero, and averaging has a negative effect since it averages out real differences. The effect on the parameter confidence interval was studied by plotting the average of the 100 coefficients of variation (cv), i.e.  $\hat{\sigma}/\hat{\beta}$  expressed as percentage. It can be seen (right hand panels) that with more observation noise the uncertainty in the parameter estimates increases with increasing

observation noise if the fields are treated as independent, and vice versa if the replicates are averaged.

The practical meaning of the results is that in experimental situations with replicates with good control over the root zone salinity, such as in greenhouses, averaging prior to estimation leads to less biased results. The practical meaning for field experiments (as carried out at e.g. SFT) can better be judged from a plot of the observation noise at a fixed target noise. In Fig. 10, a target noise of  $1 \text{ dS m}^{-1}$  is assumed, with an observation noise ranging from 0 to 3. The bias is practically absent without error-in-variables, i.e. at observation noise 0 (the small deviation is due to the randomness of the yield), and expands rapidly when the noise increases. The threshold is underestimated (negative bias), but overestimated by averaging. Beyond about  $1 \text{ dS m}^{-1}$  averaging the soil salinity per treatment group leads to lower absolute bias. As, at SFT, according to Fig. 2, the total uncertainty is generally less than  $2 \text{ dS m}^{-1}$ , there is little practical difference between averaging or not. This also holds for the slope  $S$ , whereas for the zero-observed-effect yield the bias is always less than 0.5% so that the choice about averaging has no impact.

When the same exercise is done for the vGH model, the overall picture is the same, but the bias in  $E_{Ce_{50}}$  is going up to +10%, compared to the -30% of the  $E_{Ce_{thr}}$  toward  $sdX = 3$ . Also the bias in slope parameter is more favourable (-25% in  $S$  vs -15% in  $p$ ), at the expense of a little bit more bias for  $Y_0$  (-2% vs. -4%).

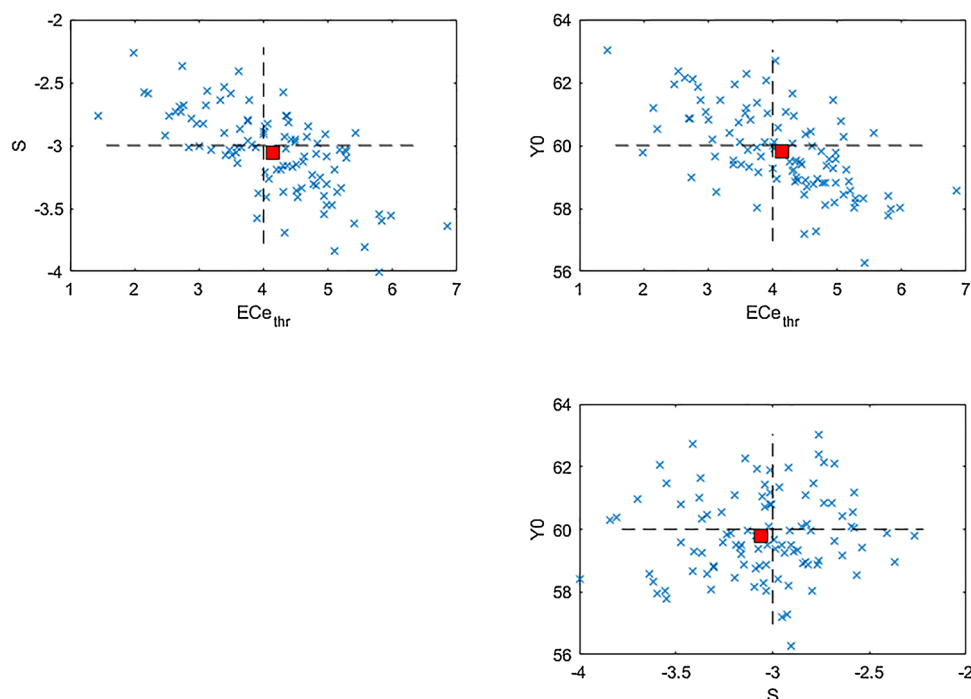


**Fig. 8.** Estimates of salt tolerance parameters for the 100 random artificial datasets with  $sdX_{target} = 1$ ,  $sdX = 2$  and  $sdY = 4$ , after taking the treatment group mean soil ECe rather than the individual field ECe.

### 3.5. An alternative agronomically sensible parameterization – $ECe_{90}$

Although the threshold ECe as parameter has been widely used, and has appeal in agricultural practice, it is doubtful whether such a sharp threshold really exists. In view of the correlations, the bias and the uncertainties, its determination from a few single experiments can only be done with large uncertainty. Moreover, there is no direct way to deduce this parameter in a decent way when the probably more realistic S-shape functions are used. Therefore, we advocate an alternative parameter that is agronomical meaningful, and can be evaluated more or less independent of the model choice. Such a parameter is the  $ECe_{90}$ , i.e. the soil ECe level at which the yield has dropped by 10%.

While the calculation of the  $ECe_{90}$  from the original parameters is straight-forward in both models, the assessment of its uncertainty is not, because there are no analytical tools for the error propagation in non-linear expressions. However, by reformulating the models such that  $ECe_{90}$  is the native parameter, the OLS can be applied to this new parameter, including the assessment of the parameter uncertainty and other statistics, completely equivalent to the procedures in Appendix A. The alternative models with  $ECe_{90}$  as parameter are presented in Appendix B.

Next, the same analysis of the effect of uncertainty on bias and estimation error is done with the new parameterization (Fig. 11). Here we chose to present the bias in absolute units ( $dS m^{-1}$ ), so that it can be compared to the estimation error.

The bias of  $ECe_{90}$  is quite a bit lower as compared to  $ECe_{thr}$ , especially at higher noise levels, and also the average estimation error is lower. This is true both for treating the fields as independent or by taking the group means.

In the vGH model (not shown), the bias in  $ECe_{90}$  is also lower than in the original parameterization with  $ECe_{50}$ , although in each case the bias almost disappears when soil salinities are averaged. The estimation error of  $ECe_{90}$  is higher though. In general, the  $ECe_{50}$  can be determined

with largest precision, which intuitively makes sense. Nevertheless, since  $ECe_{50}$  is less interesting from an agricultural point of view, it remains useful to know the confidence range for the more relevant  $ECe_{90}$ .

The robustness of determining  $ECe_{90}$  under different model assumptions was also evaluated. To this end, data were generated with the vGH model (with  $ECe_{50} = 12$ ,  $p = 3$ , so that the equivalent true  $ECe_{90} = 5.77 dS/m$ ) and  $EC_{90}$  was estimated with the alternative forms of both models. Application of the MH model mimics the situation where the data are evaluated with the popular threshold model while they originate, in fact, from an S-shape curve. Again, 100 sets were generated for three combinations of target noise and observation noise, with a total sum of 2 dS/m (illustrative of the situation at SFT).

In the absence of observation noise ( $sdX = 0$ ) there are differences between the two models (Table 3), and it requires the correct model (vGH) to obtain the correct value. While the bias increases when the observation noise ( $sdX$ ) gets larger, as expected, the estimates of both models become remarkably similar (Table 3).

It should be noted that the transformation to  $ECe_{90}$  does not modify the yield prediction uncertainty bounds as shown in Fig. 4.

### 3.6. Representation of salt tolerance by uncertainty ellipses over multiple years

The method can now be applied to data from several years of experimentation. It is already clear from the data that the estimated parameters will differ from year to year. To get an impression of the salt tolerance over the years, the uncertainty ellipses for the MH model obtained with the individual data have been plotted for the alternative form with  $ECe_{90}$  (Fig. 12).

For easier interpretation, the slope is represented here as the percentage decline per unit soil ECe change.

In some years, with the Maas-Hoffman model, it appeared not



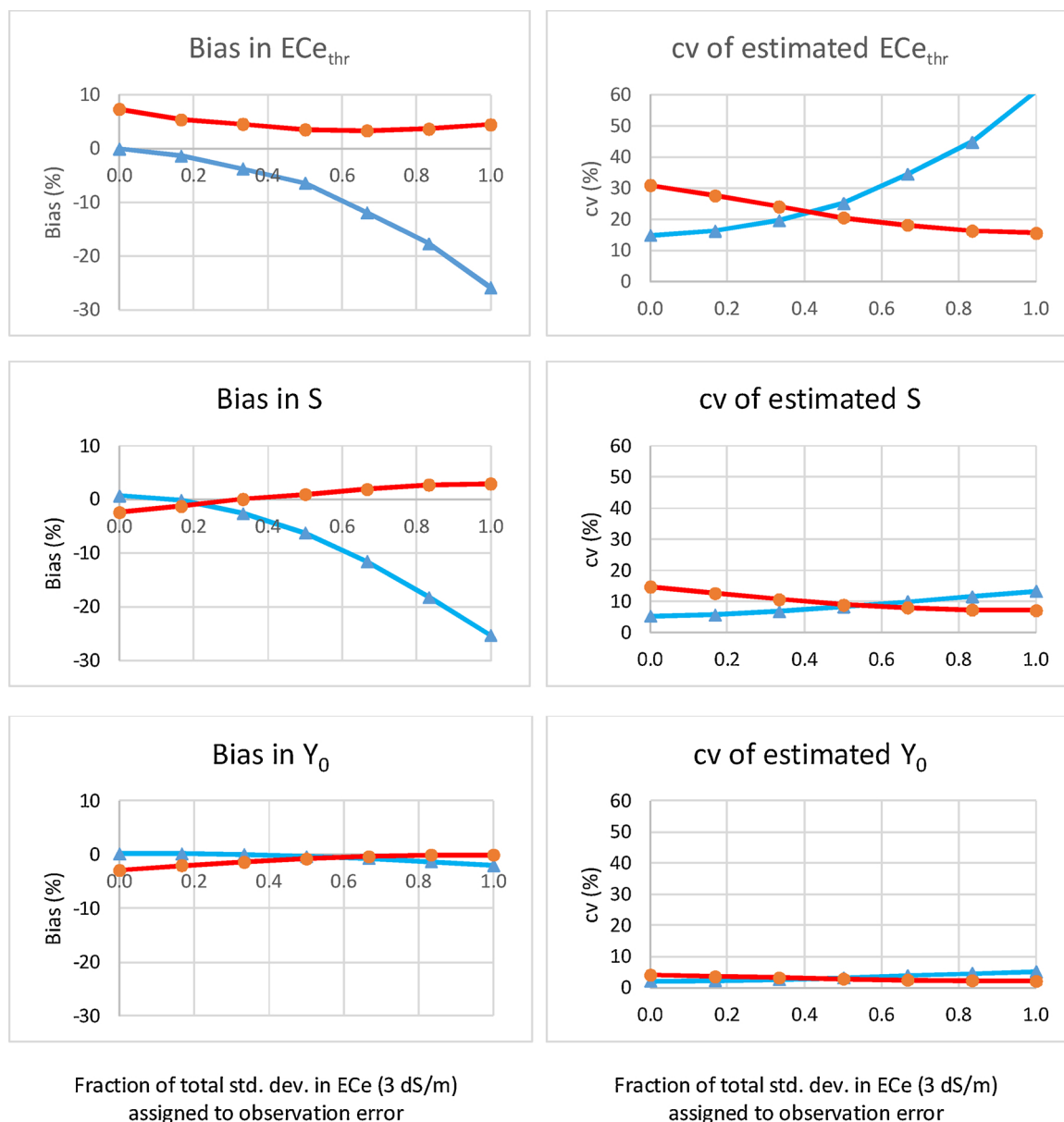


**Fig. 9.** Effect of soil salinity noise distribution over target noise and observation noise on the bias (left; a negative value means that the estimate is lower than the true value) and mean estimation error (right; expressed as coefficient of variation (cv)) in the threshold model(MH). Total noise sum is 3 dS/m. Triangles: all fields separately; Circles: with treatment group mean soil salinity.

possible to obtain a reliable estimate for the threshold ECE. The inverse in the matrix  $J^T J$  in Eq. (A.3) cannot be evaluated because the matrix is singular. It can be shown that this occurs when there are no data below the threshold ECE, so that the model cannot be distinguished from a linear regression model. This would be different if an independent measurement of the zero-observed-effect yield  $Y_0$  would be available, but this is not the case. In the vGH model the above problem does not occur, since all data contribute to the curve. Hence, to obtain approximate uncertainty bounds in the ill-conditioned case, the MH curve was directed to the  $Y_0$  found from the vGH model. This was done by adding some additional pseudo-data pairs at  $ECE = 0$  (three extra points with the vGH  $Y_0$ , and two points plus or minus one standard deviation). This procedure was tested extensively and was found to provide approximate uncertainty bounds that coincide well with the simultaneous prediction error like the one shown in Fig. 4.

The area with most overlap of the ellipsoidal regions can be considered as the most likely multi-annual estimate, thus leading to an  $ECE_{90}$  of about 5.5 dS/m with a decline rate of roughly 5.5% per dS/m. In this case, there is little difference between averaging or not over the treatment mean seasonal soil ECE (not shown).

Similar plots can be made for the vanGenuchten-Hoffman model (not shown).

#### 4. Concluding remarks

Our improved methodology to assess salt tolerance of crops resolves a number of issues in the current estimation of salt tolerance parameters from field trials. The success of our proposed method depends upon the success of the field trial and does not provide a solution for additional issues that are inherent in final-yield field trials. A common

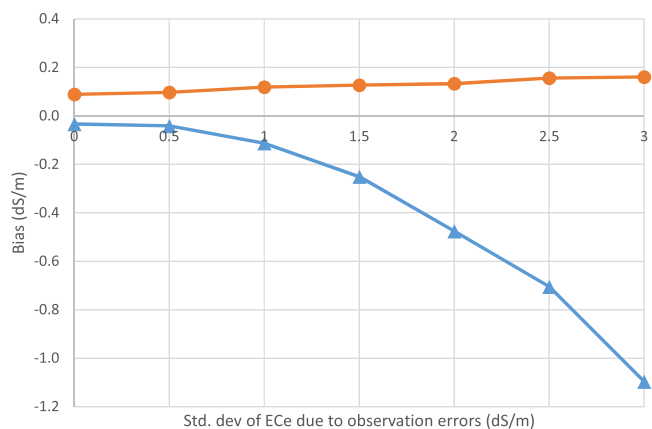


**Fig. 10.** Effect of increasing observation noise at a fixed value of the noise in target salinity of 1 dS/m. Triangles: each field independently. Circles: with the group mean ECe.

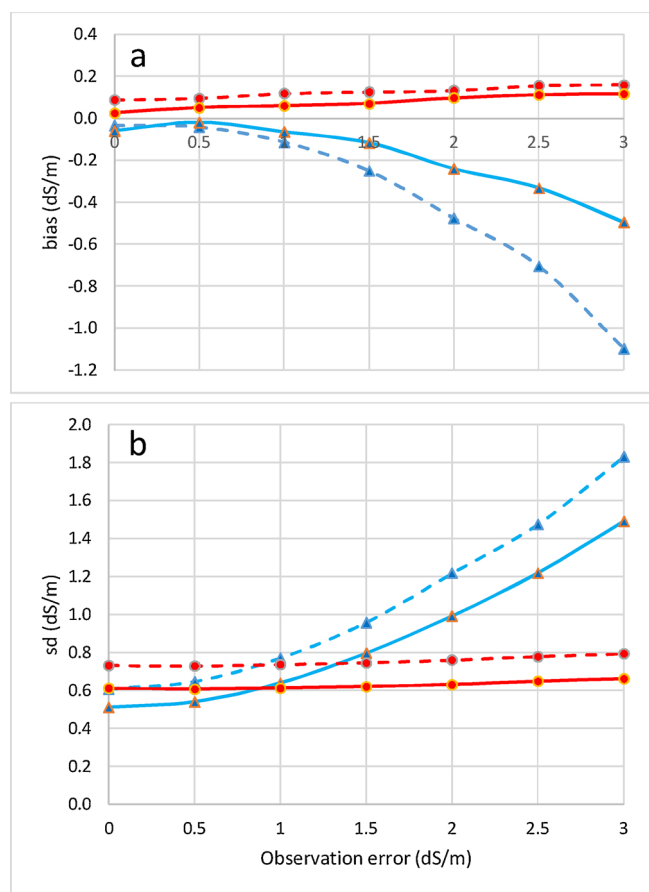


**Fig. 11.** Comparison of bias (a) and standard error (b) of  $ECe_{thr}$  and  $ECe_{90}$ . Target salinity noise fixed at 1 dS/m. Solid lines:  $ECe_{90}$ ; dashed lines:  $ECe_{thr}$ . Triangles: each replicate separately, circles: with treatment group averaged soil salinity.

prerequisites is the prevention of other limiting factors, such as water stress. In addition, variation in soil salinity during the season cannot always be avoided, but the effects are hard to investigate from final yield observations alone. The method can cope with yield variations between years, but method nor final-yield field trials can unravel the

**Table 3**

Average estimated value of  $ECe_{90}$  for data generated with the vGH model with various values of the two sources of noise in soil salinity (all in dS/m). True value 5.77 dS/m.

sdXtarget	sdX	ECe90	
		MH	vGH
2	0	5.52	5.78
1	1	5.63	5.68
0	2	5.35	5.37

causes, such as variation in breed material, differences in plant-soil interaction, differences in soil biotics, and the effect of growth stage on salinity tolerance.

With these limitations in mind we showed that the ordinary least squares method provides an objective manner to assess the salt tolerance of crops. The associated analysis of the parameter uncertainties and correlations reveals that unavoidable noise alone is already responsible for part of the variety in salt tolerance values reported in the literature, underlining the necessity to perform experiments over a number of years. In general, the zero-observed-effect yield must be considered as a parameter that needs to be estimated as well. The customary estimation from relative rather than absolute yields is prone to error, unless the reference yield  $Y_0$  is known with large precision. Efforts in the field to assess the zero-observed-effect yield will be rewarding as pin-pointing this parameter reduces the uncertainties.

The uncertainty in the soil salinity as the independent variable leads to estimation bias. The bias reduces when the proportion of the noise that cannot be explained by known variation in treatment salinity is lower. In high noise situations, the effect of bias can be mitigated by averaging the soil salinities of replicate fields with the same target salinity prior to estimation. Averaging also results in lower variance of the parameters in that case. At Salt Farm Texel the bias is relatively low. The situation in other field test sites can be readily judged by performing a similar numerical experiment. Our expectation is that in carefully designed experiments bias is not a major problem.

The parameter estimation variance obtained from a single experiment is generally a good measure of the 95% confidence bound of an ensemble of measurements, but with high soil salinity variance the reliability of the 2- $\sigma$  boundary of the slope is substantially lower.

The correlation between the estimates, for instance between zero-observed-effect yield and threshold, must be considered when judging separately reported uncertainty bounds. In calculating the prediction uncertainty of the expected yield at a specific soil salinity, our method automatically accounts for the covariance. The prediction uncertainty is smaller than when the bounds are considered independently. The plot of the ellipsoidal uncertainty ranges is offered as a convenient way to aggregate the data over multiple years. The S-shape model has better mathematical properties than the threshold model, but the  $ECe_{50}$  is a less attractive parameter in practice. On the other hand, the threshold ECe is often hard to determine, and its true existence may be questioned. As an alternative to both the  $ECe_{50}$  as well as the threshold ECe, the  $ECe_{90}$  might be a better choice. While its value can easily be obtained from original model parameters, its uncertainty cannot. It has been shown that by a simple model transformation its estimation uncertainty can be estimated. It turns out that bias and estimation variance are lower than for the threshold EC, and its estimate is more robust against the choice of the descriptive model. Hence, we advocate our method to reduce statistical issues prevailing in current estimation approaches and recommend  $EC_{90}$  as an agronomical sensible measure of salt tolerance of crops.

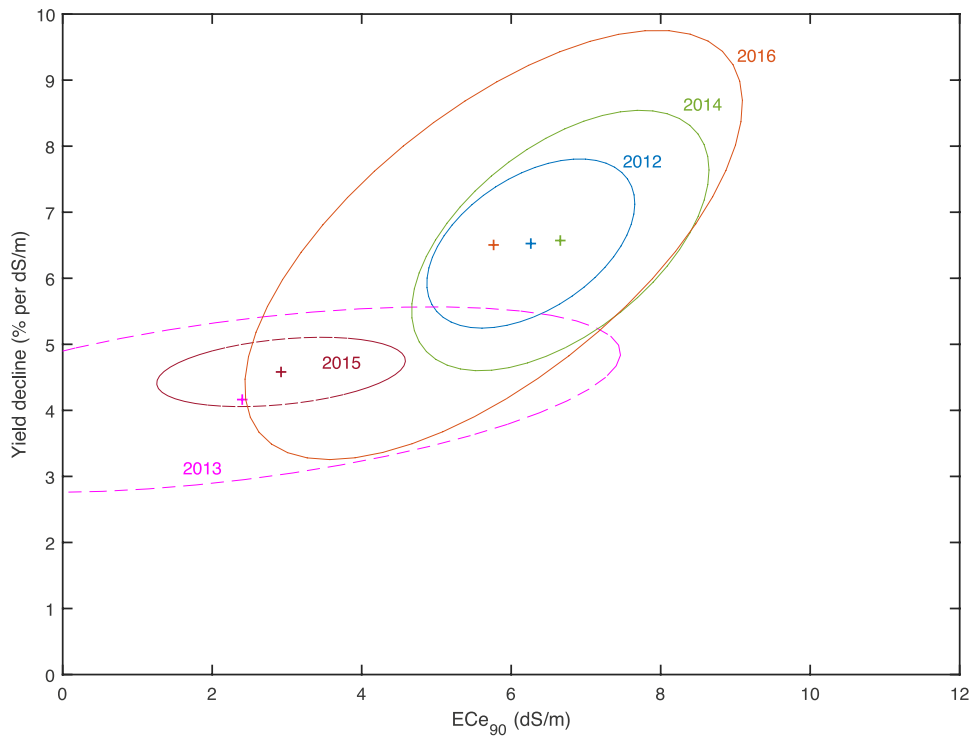


Fig. 12. Uncertainty ellipses for potato Achilles of thresholds (x-axis) and slope of yield decline (y-axis), estimated with the Maas-Hofmann model over the years 2012–2016 using the individual field data, with the alternate parameterization based on  $ECe_{90}$ . Dashed lines: ill-conditioned cases (see text).

**Acknowledgements**

We thank Prof. J. Goudriaan for critically reading earlier versions of

the manuscript. This work was supported by the Dutch Waddenfonds, the Provinces of Groningen and North-Holland, The Ministry of Agriculture, Nature and Food Quality, and the Salt Farm Foundation.

**Appendix A. Parameter estimation and co-variance assessment**

*A1 Estimation method*

The ordinary least squares method (OLS) is given by

$$\hat{\beta} = \operatorname{argmin} V(\beta) \tag{A.1}$$

where the caret denotes the estimate, and where  $V(\beta)$  is the sum of squared differences given by

$$V(\beta) = \sum_{i=1}^N (Y(i; \beta) - Y_{\text{obs}}(i))^2 \tag{A.2}$$

Here  $Y_{\text{obs}}(i)$  is the observed yield at the  $i$ -th  $ECe$  value, and  $Y(i; \beta)$  the modelled yield given by any of the models (2) or (4).

*A2 Confidence contours and intervals*

The co-variance matrix of the parameter estimates is given by

$$P = \operatorname{cov}(\hat{\beta}) = \frac{V(\hat{\beta})}{N - n_p} (J^T J)^{-1} \tag{A.3}$$

Here,  $N$  is the number of samples,  $n_p$  the number of parameters and  $J$  is the Jacobian matrix, formed by the derivatives of each output observation to the parameters. Hence,  $J$  is a  $N \times n_p$  matrix. Consequently, the covariance matrix  $P$  is a  $n_p \times n_p$  (symmetric) matrix.

The standard deviation of the estimate is

$$\sigma(\beta_j) = \sqrt{P_{jj}} \tag{A.4}$$

and the correlation coefficient for the off-diagonal elements is

$$\frac{\sigma_{12}^2}{\sigma_1 \sigma_2} \tag{A.5}$$

An approximate 95% confidence interval (Cramér-Rao lower bound) for parameter  $j$  when all other parameters are at their optimal value is

$$\hat{\beta}_j - 2\sigma(\beta_j) \leq \beta_j \leq \hat{\beta}_j + 2\sigma(\beta_j) \tag{A.6}$$

The percentage is approximate since the model is non-linear in the parameters.

Individual parameter confidence intervals can be misleading if there is correlation between the estimates. The confidence region is ellipsoidal, and the corner points of the region defined by Eq. (C.6) are usually outside the confidence region.

Expression (A.3) requires the inversion of the  $n_p \times n_p$  matrix  $J^T J$ . This inversion is possible only when the matrix is well conditioned. The condition number is the ratio between the largest and smallest eigenvalue of this matrix. When the condition number is large the matrix inversion becomes problematic, and the covariance of the parameters blows up. In that case, no reliable parameter estimates can be obtained.

**A3 Prediction error**

The non-simultaneous prediction error specifies the uncertainty of prediction of the yield when one additional ECe were tested. It is given by

$$b_{ns}(i) = 2 \sqrt{\frac{V(\hat{\beta})}{N - n_p} + J(i, :)PJ(i, :)^T} \tag{A.7}$$

where  $J(i, :)$  is the  $i$ -th row of the  $N \times n_p$  Jacobian matrix, and  $P$  the covariance matrix according to Eq. (A.3). The predicted yield is expected with approximately 95% confidence between the bounds  $Y(\hat{\beta}; i) - b_{ns}(i)$  and  $Y(\hat{\beta}; i) + b_{ns}(i)$ .

The simultaneous prediction error is given by

$$b_s(i) = 2 \sqrt{J(i, :)PJ(i, :)^T} \tag{A.8}$$

It represents the bounds of the curve when measurements for all ECe values would be repeated. It is important to remark that this does not mean that the curve in another year will be within this bound. The predicted values are between the bounds  $Y(\hat{\beta}; i) - b_s(i)$  and  $Y(\hat{\beta}; i) + b_s(i)$ .

It can be seen from Eqs. (A.7) and (A.8) that the simultaneous prediction error is smaller than the non-simultaneous prediction error.

**A4 Goodness of fit**

Root mean square error

$$rmse = \sqrt{\frac{V(\hat{\beta})}{N - n_p}} \tag{A.9}$$

Number of degrees of freedom

$$dof = N - n_p \tag{A.10}$$

R-square

$$R^2 = 1 - \frac{V(\hat{\beta})}{\sum_{i=1}^N (Y_{obs}(i) - \bar{Y}_{obs}(i))^2} \tag{A.11}$$

Adjusted R-square

$$R^2 = 1 - \frac{\frac{1}{N - n_p} V(\hat{\beta})}{\frac{1}{N - 1} \sum_{i=1}^N (Y_{obs}(i) - \bar{Y}_{obs}(i))^2} \tag{A.12}$$

Closer to 1 is better.

Akaike's Information Criterion AIC

$$AIC = 2n_p + N \ln(V(\hat{\beta})) \tag{A.13}$$

Based on the likelihood but ignoring the constant term  $-N \ln(N) - N \ln(2\pi) - N$ . The model with the lowest AIC is preferred.

**Appendix B. Alternate model formulation with ECE<sub>nn</sub>**

The derivation is done for any desired percentage  $nn$  % of residual yield at ECE<sub>nn</sub>, where  $0 < nn < = 100$ .

**Maas-Hoffman**

At the desired  $ECE_{nn}$  the following holds

$$\frac{Y\{ECE_{nn}\}}{Y_0} = \frac{nn}{100} = 1 + \frac{S}{Y_0} * (ECE_{nn} - ECE_{thr}) \tag{B.1}$$

From this expression  $ECE_{thr}$  can be expressed in the new parameter, i.e.

$$ECE_{thr} = ECE_{nn} + f_{nn} \frac{Y_0}{S} \tag{B.2}$$

where  $f_{nn}$  is a constant given by

$$f_{nn} = \frac{100 - nn}{100} \tag{B.3}$$

Substitution in the original model now gives the alternative MH model:

$$\frac{Y}{Y_0} = \begin{cases} 1 & ECe \leq ECe_{nn} + f_{nn} \frac{Y_0}{S} \\ 1 - f_{nn} + \frac{S}{Y_0} * (ECe - ECe_{nn}) & ECe_{nn} + f_{nn} \frac{Y_0}{S} < ECe < ECe_{nn} + (f_{nn} - 1) \frac{Y_0}{S} \\ 0 & ECe > ECe_{nn} + (f_{nn} - 1) \frac{Y_0}{S} \end{cases} \quad (B.4)$$

At  $nn = 100$   $f_{nn} = 0$  and  $ECe_{nn} = ECe_{thr}$ , which yields the original model. The choice  $nn = 0$  formulates the model in terms of  $Y_0$ ,  $S$  and the lethal soil salinity  $ECe_{lethal}$ .

van Genuchten-Hoffman

$$\frac{Y\{ECe_{nn}\}}{Y_0} = \frac{nn}{100} = \frac{1}{1 + \left(\frac{ECe_{nn}}{ECe_{50}}\right)^p} \quad (B.5)$$

Hence

$$(ECe_{nn})^p = (ECe_{50})^p g_{nn} \quad (B.6)$$

where  $g_{nn} = f_{nn} \frac{100}{nn}$ .

To be meaningful, it is required that  $0 < nn < 100$ .

Substitution in the original model yields the alternate form of the vGH model:

$$\frac{Y}{Y_0} = \frac{1}{1 + g_{nn} \left(\frac{ECe}{ECe_{nn}}\right)^p} \quad (B.7)$$

At  $nn = 50$   $g_{nn} = 1$  thus providing the original model.

## References

- De Pascale, S., Barbieri, G., 1995. Effects of soil salinity from long-term irrigation with saline-sodic water on yield and quality of winter vegetable crops. *Sci. Hortic.* 64, 145–157.
- De Vos, A., Bruning, B., van Straten, G., Oosterbaan, R., Rozema, J., van Bodegom, P., 2016. Crop Salt Tolerance Under Controlled Field Conditions in the Netherlands, Based on Trials Conducted at Salt Farm Texel. Salt Farm Texel, Den Hoorn, Texel (Accessed 1 March 2018). <https://www.saltfarmtexel.com/publications>.
- Ghassemi, F., Jakeman, A.J., Nix, H.A., 1995. *Salinization of Land and Water Resources: Human Causes, Extent, Management and Case Studies*. University of NSW, Sydney 526 pp.
- Groenvelde, T., Ben-Gal, A., Yermiyahu, U., Lazarovitch, N., 2013. Weather determined relative sensitivity of plants to salinity: quantification and simulation. *Vadose Zone J.* 12.
- Maas, E.V., 1993. Testing crops for salinity tolerance. In: Manville, B.V.B.J.W., Duncan, R.R., Yohe, J.M. (Eds.), *INSTORMIL*. University of Nevada, Lincoln, NE, USA, pp. 234–247.
- Maas, E.V., Hoffman, G.J., 1977. Crop salt tolerance - current assessment. *ASCE J. Irrig. Drain Div.* 103, 115–134.
- Qadir, M., Quillerou, E., Nangia, V., Murtaza, G., Singh, M., Thomas, R.J., Crechsel, P., Noble, A.D., 2014. Economics of Salt-Induced Land Degradation and Restoration. United Nations <https://doi.org/10.1111/1477-8947.12054>.
- Rozema, J., Flowers, T., 2008. Crops for a salinized world. *Science* 322, 1478–1480.
- Rozema, J., Cornelisse, D., Zhang, Y., Li, H., Bruning, B., Katschnig, D., Broekman, R., Ji, B., van Bodegom, P., 2015. Comparing salt tolerance of beet cultivars and their haplophytic ancestor: Consequences of domestication and breeding programmes. *AoB Plants* 7 (1). <https://doi.org/10.1093/aobpla/plu083>. plu083.
- Sadeh, A., Ravina, I., 2000. Relationships between yield and irrigation with low-quality water — a system approach. *Agric. Syst.* 64, 99–113.
- Shani, U., Dudley, L.M., 2001. Field studies of crop response to water and salt stress. *Soil Sci. Soc. Am. J.* 65, 1522–1528.
- Stuyt, L.C.P.M., Blom-Zandstra, M., Kselik, R.A.L., 2016. Inventarisatie en analyse zout-tolerantie van landbouwgewassen op basis van bestaande gegevens (Inventory and Analysis of Salt Tolerance of Agricultural Crops from Existing Data). Rep. No. 2739. Wageningen, The Netherlands (in Dutch). <http://library.wur.nl/WebQuery/wurpubs/508610>.
- Ulery, A.L., Teed, J.A., Van Genuchten, M.T., Shannon, M.C., 1998. SALTDATA: a database of plant yield response to salinity. *Agron. J.* 90, 556–562.
- van Genuchten, M.T., Gupta, S.K., 1993. A reassessment of the crop tolerance response function. *J. Indian Soc. Soil Sci.* 41, 730–737.
- Van Genuchten, M.T., Hoffman, G., 1984. Analysis of crop salt tolerance data. In: Shainberg, I., Shalhevet, J. (Eds.), *Soil Salinity under Irrigation - Process and Management*. Vol. Ecological Studies. Springer Verlag, Berlin, pp. 258–271.
- Van Straten, G., De Vos, A., Vlaming, R., Oosterbaan, R., 2016. Field tests of dielectric sensors in a facility for studying salt tolerance of crops. *Int. Agric. Eng. J.* 25, 102–113.